

Nonlinear optical absorption of semiconductor quantum wires: Photoexcitation dynamical effects

Justino R. Madureira

Instituto de Física, Universidade Estadual de Campinas, CP 6165, 13083-970 Campinas-SP, Brazil

Marcos H. Degani

Haras Degani, Ave Fioravante Piovani 1000, 13250-000 Itatiba-SP, Brazil

Marcelo Z. Maialle

Liceu Vivere, Rua Duque de Caxias Norte 550, 13635-000 Pirassununga-SP, Brazil

(Received 4 April 2003; revised manuscript received 17 July 2003; published 8 October 2003)

We investigate the optical absorption spectra of semiconductor quantum wires and its dependence on the optical pumping power. The absorption coefficient is obtained solving the semiconductor Bloch equations in the real-space and time domains, including corrections due to band-gap renormalization, local field, and screening. We find that the energy shifts in the spectra due to increasing photoexcitation power have different behavior when treating dynamically the carrier creation rather than using stationary carrier distribution at thermal equilibrium. Dealing with the nonequilibrium distribution dynamically, we are able to describe the observed constancy of the peak position of the fundamental transition energy with the optical pumping power. The competing effects of the dynamical band-gap renormalization and the local-field correction leads to an almost cancellation of the red/blue shift energy.

DOI: 10.1103/PhysRevB.68.161301

PACS number(s): 78.67.-n, 85.35.Be, 71.35.-y

Quantum wire structures have attracted much attention due to their distinct optical and electronic properties which have potential applications in novel optoelectronic devices.^{1,2} One type of quantum wire that has been successfully grown is the so-called *T* wire,³ where the electronic states are localized at the intersection of two crossing quantum wells. In tilted *T* wire, for which the stem and arm wells are not orthogonal ($\theta \neq 90^\circ$, see Fig. 1), it is possible to grow larger active areas needed for technological applications in devices having stronger response.⁴

In this work we study the optical absorption of a tilted *T* wire. We investigate the influences of the optical pumping power on the optical absorption spectrum via the band-gap renormalization, the local-field effect, and the screening in the effective one-dimensional (1D) Coulomb interaction.⁵⁻⁸ The latter was obtained performing an average of the 3D Coulomb interaction with the lateral carrier states calculated numerically from the 2D Schrödinger equation. We consider the carrier occupation, in the semiconductor Bloch equation (SBE),^{7,9} as a nonequilibrium distribution, which is created dynamically in the system. We have found that it plays an important role, through the phase-space filling, the renormalization gap, and the local-field term in SBE, on the behavior of the peak position of the fundamental energy transition, i.e., the observed experimental¹¹ red/blue shift compensation of the optical absorption spectra. This fact has also been explained by Das Sarma and Wang,¹² solving the Bethe-Salpeter equation for a *T*-shaped quantum wire. They have found that the independence of the peak position with respect to the optical pumping power can only be explained considering dynamical screening in the Coulomb interaction, albeit using a carrier distribution in thermal equilibrium.

The optical absorption is calculated from the interband polarization whose time evolution equation is given by the SBE. We work within the relaxation-time approximation

since our main interest is on the coherent excitation dynamics that takes place in femtosecond scale. We also consider the case of resonant excitation, such that only the lowest conduction and the highest valence subbands of the quantum wire participate. The space-time evolution of the interband optical polarization $P(z,t)$ and the nonequilibrium carrier population $n_e(z,t) = n_h(z,t) = n(z,t)$ are given by^{7,9,10,13}

$$\begin{aligned}
 i\hbar \frac{\partial}{\partial t} P(z,t) = & H P(z,t) + d_0 E(t) [2n(z,t) - L\delta(z)] \\
 & - \frac{1}{L} \int dz' [V^{hhhh}(z') + V^{eeee}(z')] n(z',t) \\
 & \times P(z-z',t) + \frac{2}{L} \int dz' V^{ehhe}(z') \\
 & \times n(z-z',t) P(z',t), \quad (1)
 \end{aligned}$$

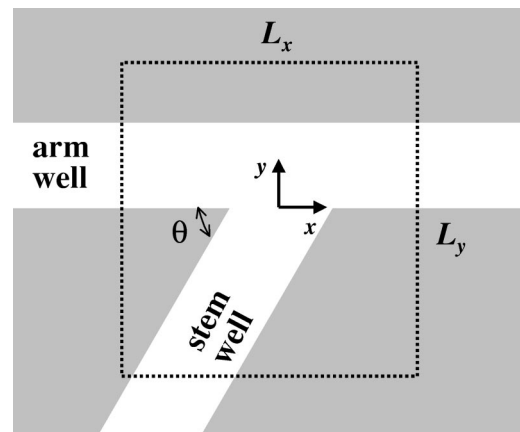


FIG. 1. Cross section of the *T*-wire system. The unit-cell region used in the numerical calculation is demarcated by the dotted lines.

$$i\hbar \frac{d}{dt} n(z,t) = P(z,t)E^*(t)d_0^* - P^*(-z,t)E(t)d_0 - \frac{1}{L} \int dz' V^{ehhe}(z') [P(z-z',t)P^*(-z',t) - P^*(z'-z,t)P(z',t)], \quad (2)$$

$$H = -\frac{\hbar^2}{2m_r} \frac{d^2}{dz^2} - V^{ehhe}(z) + \tilde{E}_g - i\hbar\Gamma, \quad (3)$$

where the effective band gap $\tilde{E}_g = E_g + E_0^e - E_0^h$ is given by the material band gap E_g and the lateral ground-state energies of electron and hole. The quantity L is the wire length, $z = z_h - z_e$ the electron-hole relative coordinate along the wire, m_r the electron-hole reduced mass ($m_r^{-1} = m_e^{-1} + m_h^{-1}$), and the optical pulse is $E(t) = E_0 e^{-i\omega_0 t} \exp\{-(4/\sigma^2)t^2\}$. The optical pumping power is calculated from $\bar{U} = \sqrt{2\pi\epsilon_0} c |E_0|^2 \sigma / 4$, given in J/cm^2 . The relaxation rate Γ accounts, within the relaxation-time approximation, for scattering processes causing dephasing of the optical polarization. The second term on the right-hand side of Eq. (1) gives the phase-space filling which bleaches the optical absorption for increasing optical pumping power. The third term is the exchange correlation that induces band-gap renormalization and the last term is the local field.

The 1D Coulomb interaction is obtained performing the average of the 3D Coulomb interaction with the lateral ground state, namely,

$$V^{\lambda\lambda'\lambda''\lambda'''}(z) = \frac{e^2}{4\pi\epsilon} \int \frac{d^2x_\lambda y_\lambda d^2x_{\lambda'} y_{\lambda'} |\phi_0^{\lambda''}|^2 |\phi_0^{\lambda'''}|^2}{\sqrt{z^2 + (x_\lambda - x_{\lambda'})^2 + (y_\lambda - y_{\lambda'})^2}}, \quad (4)$$

where $\lambda, \lambda' = e, h$ for electron e and hole h . The lateral ground states are given by the solution of the 2D Schrödinger equation with the potential given by band-gap differences of the materials in the heterostructure.

The absorption coefficient is obtained from the total polarization $P(z=0,t)$ in the usual way calculating the complex dielectric function,⁹ namely,

$$\alpha(\omega) = \frac{\omega}{c} \frac{\epsilon''(\omega)}{\left(\frac{1}{2} \{ \epsilon'(\omega) + \sqrt{[\epsilon'(\omega)]^2 + [\epsilon''(\omega)]^2} \} \right)^{1/2}}, \quad (5)$$

where the real and imaginary part can be obtained from the solution of the SBE, Eqs. (1)–(3), i.e.,

$$\epsilon'(\omega) = \text{Re}\{\epsilon(\omega)\} = \epsilon_{bg} + \text{Re}\left\{ \frac{P(\omega)}{\mathcal{V}\epsilon_0 E(\omega)} \right\}, \quad (6)$$

$$\epsilon''(\omega) = \text{Im}\{\epsilon(\omega)\} = \text{Im}\left\{ \frac{P(\omega)}{\mathcal{V}\epsilon_0 E(\omega)} \right\}. \quad (7)$$

We have investigated a T -wire system made of GaAs/Al_{0.3}Ga_{0.7}As semiconductors for which the electron ef-

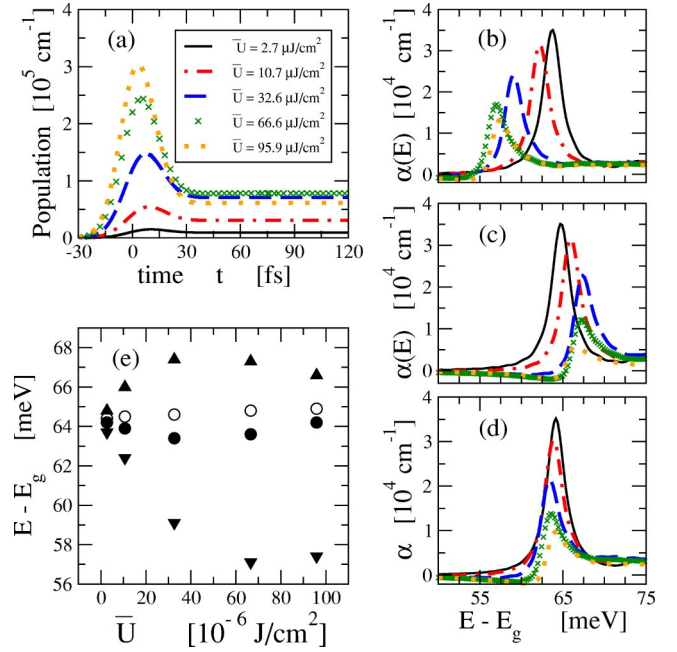


FIG. 2. (Color online) (a) Carrier density as a function of time for different intensities of the optical pumping pulse. Panels (b–d) show the optical-absorption spectra for different intensities of the pulse. Rest is the same as in panel (a). In (b) we have switched off the local field—last term of Eq. (1); in (c) we have switched off only the band-gap renormalization—third term of Eq. (1); and in panel (d) we have considered full Eq. (1). Panel (e) shows the exciton peak energy as a function of the intensity of the pumping pulse; triangle down corresponds to panel (b), triangle up corresponds to panel (c), full circle corresponds to panel (d), and empty circle denotes exciton energy switching off band-gap renormalization and local field.

fective mass $m_e = 0.067m_0$ and anisotropic heavy-hole masses $m_{hx} = m_{hz} = 0.13m_0$ and $m_{hy} = 0.34m_0$, with m_0 being the free-electron mass. The effective masses are considered to be the same for the well and barrier materials. The potential barriers, due to band-gap energy difference of the materials, are $V^e = 219.7$ meV for the conduction electron and $V^h = 134.6$ meV for the valence heavy hole. The background dielectric constant is $\epsilon_{bg} = 13.1$, ϵ_0 is the vacuum dielectric constant, and the interband dipole moment is $d_{cv} = 0.3$ e nm. The system investigated is a tilted T wire⁴ ($\theta = 30^\circ$) with the arm and stem quantum wells of widths 5.0 nm. An unitary cell representing the system (Fig. 1), of sizes $L_x = 768$ nm and $L_y = 240$ nm, was used in the calculation of the lateral states.

The time propagation scheme of Eqs. (1)–(3) was implemented numerically¹⁴ using time discretization $\Delta t = 0.07$ fs with a total of 17 000 points and a discretized relative e - h distance with intervals of $\Delta z = 0.35$ nm using 6000 points. The optical pumping pulse was assumed to be a Gaussian with a width $\sigma = 40$ fs and frequency centered at the material band gap, i.e. $\hbar\omega_0 = 1520$ meV. The dephasing time in all calculations is $\Gamma = 500$ fs.^{9,13,15}

Figure 2 presents the nonequilibrium carrier population and the optical-absorption spectra for different mean values

of the optical pumping power. Figure 2(a) shows the density of carriers, $\Sigma_k n_k(t) = n(z=0, t)$, obtained from Eq. (2), as a function of time. Its initial time oscillation is due to the generalized Rabi oscillation that takes place while the optical pulse is inside the system. After that the carrier population becomes a nonequilibrium stationary distribution for a long period of time (≈ 1.5 ps). Here we have not addressed processes that bring this population to equilibrium since we are presently concerned only with the coherent initial dynamics. The spectra for low power [full line in Figs. 2(b)–2(d)] are essentially the same, considering or not the integral terms in the SBE. Figure 2(b) shows the influence of the band-gap renormalization (switching off the local field), i.e., a redshift of the optical-absorption spectrum. Figure 2(c) shows an opposite effect due to the local-field effect (in absence of band-gap renormalization), that is a blue shift. Summing up both effects, they almost cancel out. It is presented in Fig. 2(d). If we switch off both the effects and increase the optical pumping power, we get a very small blue shift of the spectra. That is due solely to the phase-space filling. We plot in Fig. 2(e) the peaks of absorption spectra showing clearly this previous discussion: the band-gap renormalization effect [triangle down, from Fig. 2(a)], local-field effect [triangle up, from Fig. 2(b)], full semiconductor equation [full circle, from Fig. 2(c)], and with empty circle we denote the peak position when we do not consider any integrals in Eqs. (1)–(3). Notice that both results (full and empty circles), for the complete and the simple (only phase-space filling and dynamical nonequilibrium carrier population) SBE, predict that the peak position of the energy of fundamental optical transition is almost independent of the optical pumping power.

As a matter of fact, photoluminescence experiment carried out on quantum wires¹¹ indirectly indicates that the absorption peak position does not depend on the optical pumping power. This fact has also been described by Das Sarma and Wang¹² using another scheme, Bethe-Salpeter equation, where they have included band-gap renormalization effect and a dynamical screening in the Coulomb interaction. The carrier population was considered in equilibrium with the thermal bath, i.e., a Fermi-Dirac distribution. They have shown that increasing the carrier density (which is similar to increasing the photoexcitation power) and considering static screening, the spectra present a red shift. When dynamical screening is taken into account, the fundamental absorption peak position is almost independent of optical pumping power, which led the authors to infer about the importance of dynamical screening.

In our scheme, the nearly vanishing energy shift is due to the dynamical excitation, which creates a nonequilibrium population [Fig. 2(a)], affecting the local field (blue shift) and band-gap renormalization (red shift) contributions in the SBE.

To evidence the effects of the dynamical photoexcitation, we consider stationary population $n(z)$ (Fermi-Dirac distribution), instead of the nonequilibrium carrier population, in Eq. (1). We have performed the calculation assuming the carrier distribution in equilibrium with the thermal bath at

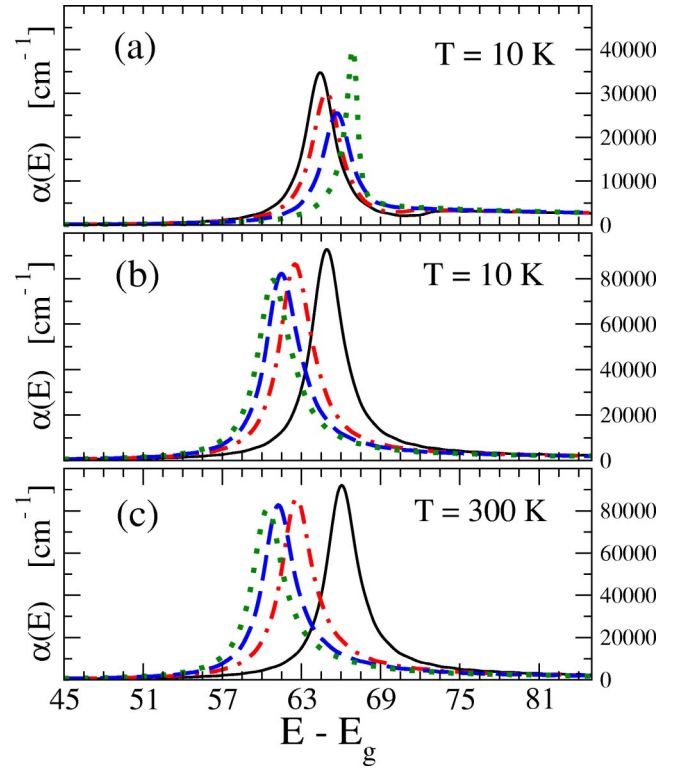


FIG. 3. (Color online) Optical-absorption spectra considering Fermi-Dirac carrier distribution in Eq. (1) at temperature T . Full line is for pumping power $\bar{U} = 2.22 \mu\text{J}/\text{cm}^2$, dot-dashed line $\bar{U} = 10.65 \mu\text{J}/\text{cm}^2$, dashed line $\bar{U} = 20.14 \mu\text{J}/\text{cm}^2$, and dotted line for $\bar{U} = 32.62 \mu\text{J}/\text{cm}^2$. In panel (a) no screening, in panels (b) and (c) with static screening and Coulomb-hole term.

temperature $T = 10$ K. These optical-absorption spectra, shown in Fig. 3(a), present a blue shift as the photoexcitation power is increased.

We have also considered in the SBE a statically screened Coulomb interaction $V_S(k) \equiv V_s(k, \omega = 0) = V(k)/\epsilon(k, \omega = 0)$, where the dielectric function, within the dynamical plasmon pole approximation, is given by^{16,12}

$$\frac{1}{\epsilon(k, \omega)} = 1 + \frac{\omega_{pl}^2(k)}{(\omega + i\delta) - \omega_k^2}, \quad (8)$$

with the 1D plasmon oscillator strength $\omega_{pl}(k) = \sqrt{nLV(k)k^2/m_r}$ and the effective plasmon frequency is given by

$$\hbar^2 \omega_k^2 = \hbar^2 \omega_{pl}^2(k) + \frac{2n}{\kappa} \frac{\hbar^2 k^2}{2m_r} + \left(\frac{\hbar^2 k^2}{2m_r} \right)^2, \quad (9)$$

where κ is the inverse screening length. The constant Coulomb-hole term is also considered: $\vec{E}_g \rightarrow \vec{E}_g + \sum_k [V_S(k) - V(k)] = E_g + V_S(z=0) - V(z=0)$. The optical-absorption spectra are shown in Fig. 3(b) with the carrier distribution (Fermi-Dirac) at equilibrium with the thermal bath at temperature $T = 10$ K. As expected, we obtain a red shift for increasing carrier concentration, as in the previous results of Das Sarma and Wang.¹² Both figures, Figs. 3(a) and 3(b),

show that the optical spectrum depends strongly on the screening, differently from what is shown by the results of Ref. 16. We have also checked that even when we consider the carrier population hotter ($T=300$ K) than the thermal bath, the Fermi-Dirac distribution assumption fails to describe the experimentally observed red/blue shift compensation.

During the optical pulse, the density of carrier reaches a maximum value, decreases, and becomes stationary. Had we used this nonequilibrium stationary population to describe the time evolution of the optical polarization, Eq. (1), we would still have obtained the red/blue shift compensation. Therefore, the *crucial* ingredient behind the determination of the peak position is the nonequilibrium nature of the carrier distribution, *not* its time dependence. Of course, in order to get this nonequilibrium distribution one needs to solve for the time dependence. The absorption coefficient calculated using this stationary distribution would be larger than the one obtained using the full dynamical carrier population. The high density of carriers, during the pulse [cf. Fig. 2(a)], increases the phase-space filling, bleaching the optical absorption. We compare in Fig. 4 our stationary nonequilibrium carrier population for average optical pumping power $\bar{U}=32.62 \mu\text{J}/\text{cm}^2$, in relative coordinates, with the Fermi-Dirac distribution. They clearly differ qualitatively. The curves for lower power, used also to obtain the spectra shown in Fig. 3, present a similar feature.

In conclusion, we have investigated different contributions, within the semiconductor Bloch equation scheme, responsible for the bleaching and shift of the optical absorption spectrum of quantum wires, namely (i) phase-space filling, (ii) the band-gap renormalization, (iii) the local-field effect, and (iv) the static screening. In addition, the equilibrium and nonequilibrium carrier distributions and their influences on

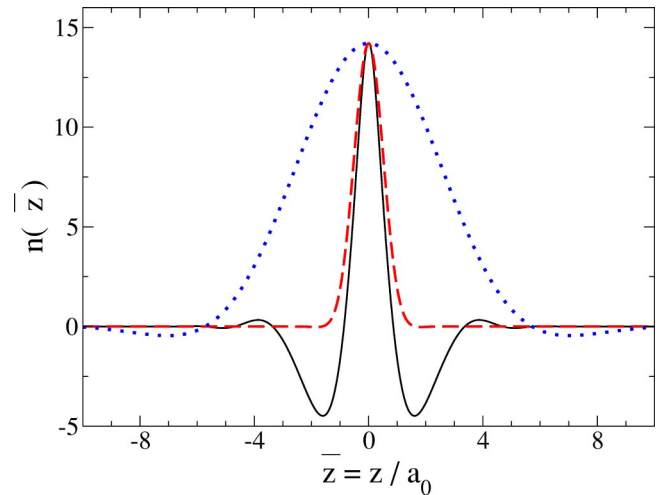


FIG. 4. (Color online) Carrier distribution as a function of the renormalized relative coordinate $\bar{z}=z/a_0$. All three distributions give the same number of electron-hole pairs per centimeter, i.e., $n(\bar{z}=0)/L$. Full lines denote stationary distribution from SBE, Eqs. (1)–(3), using the average optical pumping power $\bar{U}=32.62 \mu\text{J}/\text{cm}^2$; dot lines denote Fermi-Dirac distribution at $T=10$ K; and dashed lines for Fermi-Dirac at $T=300$ K.

the dynamics of points (i)–(iii) are investigated. We found that the peak position of the fundamental optical transition is strongly dependent on these contributions and on the carrier distribution. The latter plays clearly a crucial role in the description of the red/blue shift compensation of the optical absorption spectrum in quantum wires.

We acknowledge helpful discussions with F. Iikawa. This work was supported in part by the São Paulo State Agency—FAPESP.

¹F. Rossi and T.F. Kuhn, *Rev. Mod. Phys.* **74**, 895 (2002).

²J. Shah, *Ultrafast Spectroscopy of Semiconductors and Semiconductors Nanostructures* (Springer, Berlin, 1998).

³L.N. Pfeiffer, K.W. West, H.L. Stormer, J.P. Eisenstein, K.W. Baldwin, D. Gershoni, and J. Spector, *Appl. Phys. Lett.* **56**, 1697 (1990); Y.C. Chang, L.L. Chang, and L. Esaki, *ibid.* **47**, 1324 (1985).

⁴N. Tomita *et al.*, *J. Vac. Sci. Technol. B* **14**, 3550 (1996); **16**, 575 (1998).

⁵S. Schmitt-Rink, D.S. Chemla, and H. Haug, *Phys. Rev. B* **37**, 941 (1988).

⁶S. Glutsch and F. Bechstedt, *Phys. Rev. B* **44**, 1368 (1991); S. Glutsch, F. Bechstedt, and D.S. Chemla, *Superlattices Microstruct.* **22**, 31 (1997).

⁷F. Rossi and E. Molinari, *Phys. Rev. Lett.* **76**, 3642 (1996); *Phys. Rev. B* **53**, 16462 (1996).

⁸F. Tassone and C. Piermarocchi, *Phys. Rev. Lett.* **82**, 843 (1999);

C. Piermarocchi and F. Tassone, *Phys. Rev. B* **63**, 245308 (2001).

⁹H. Haug and S. W. Koch, *Quantum Theory of the Optical and Electronic Properties of Semiconductors*, 3rd ed. (World Scientific, Singapore, 1994).

¹⁰M. Bonitz, *Quantum Kinetic Theory* (Tuebner, Stuttgart, 1998).

¹¹W. Wegscheider *et al.*, *Phys. Rev. Lett.* **71**, 4071 (1993); R. Ambigapath, I. Bar-Joseph, D.Y. Oberli, S. Haacke, M.J. Brasil, F. Reinhardt, E. Kapon, and B. Deveaud *ibid.* **78**, 3579 (1997).

¹²D.W. Wang and S. Das Sarma, *Phys. Rev. B* **64**, 195313 (2001); S. Das Sarma and D.W. Wang, *Phys. Rev. Lett.* **84**, 2010 (2000).

¹³J.R. Madureira, M.Z. Maialle, and M.H. Degani, *Phys. Rev. B* **66**, 075332 (2002).

¹⁴M.H. Degani, *Appl. Phys. Lett.* **59**, 57 (1991).

¹⁵S. Hughes and D.S. Citrin, *Phys. Rev. Lett.* **84**, 4228 (2000); S. Hughes, *Phys. Rev. B* **63**, 153308 (2001).

¹⁶S. Benner and H. Haug, *Europhys. Lett.* **16**, 579 (1991).